On the Motion of a Bubble through Microchannel Contractions

Henry Chio*, Mads Jakob Jensen**, Xiaolin Wang*, Henrik Bruus**, and Daniel Attinger***

*State University of New York, Stony Brook NY 11794-2300
**Technical University of Denmark, DK-2800 Kongens Lyngby
***Columbia University, New York NY 10027, da2203@columbia.edu

ABSTRACT

We present the first transient pressure measurements and high-speed visualization of gas bubbles passing through liquid-filled microchannel contractions. We have studied contractions ranging from 100 to 500 µm in glass tubes of main diameter 2 mm and compared the experimental results with a recent model of quasi-stationary bubble motion [1]. Transient pressure measurements, bubble deformations, and the influence of the bubble length on the so-called clogging pressure ΔP_c are shown to be in good agreement with the model, both in terms of maximum values and transient evolution. Some deviations from the model are also observed and possible reasons for this are investigated, such as contact line pinning, thin liquid film along the bubble and capillary instabilities. We also propose a criterion based on a modified capillary number to discriminate between two flow regimes: a quasi-stationary regime for low capillary number, and a viscosity-influenced regime for non-negligible capillary numbers.

Keywords: bubble, micro-channel, pressure drop, contraction

1 INTRODUCTION

In a typical microfluidic system [2], the fluid flows into channels with diameters ranging from 3 mm to 50 µm, along a path involving multiple branching and contractions. Materials range from ceramic and stainless steel, to polymer (PTFE, Tygon, Peek) and silicon, each having different wetting properties. In several cases, the functionality of a microfluidic system relies on the presence of gas bubbles such as micropumps using bubbles as actuators [3] and devices creating controlled liquid-gas emulsions [4, 5]. In other cases unwanted bubbles appear due to cavitation, electrochemistry, or priming (filling) of the microchannels: they become problematic if they get stuck in contractions present in the microfluidic system. For instance, when a bubble is stuck in a corner or in a dead flow zone, it can be extremely difficult to dislodge it, resulting in a reduction in dynamic performance or accuracy of the microfluidic device. Therefore, an entire batch of MEMS microfluidics devices can be ruined by only one problematic geometric feature. These problems were already identified a decade ago [6, 7] , but were not studied in depth before the problem was picked by Jensen, Goranovic, and Bruus in a recent theoretical study [1].

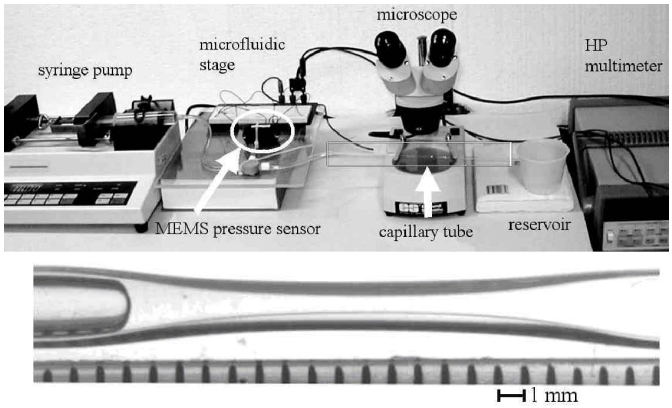

Figure 1: (top) Measurement setup allowing for transient visualization and pressure measurement during the transport of a microbubble in a microchannel. (bottom) Bubble entering the contraction of tube A7.

2 EXPERIMENTAL SETUP

For the experimental part of the work capillary glass tubes of circular cross section were used, see table 1. The tubes with contractions as shown in Figure 1 were manufactured in the glass shop of Stony Brook University.

ID	D [mm]	d [μm]	L [mm]	ΔP_c^m [Pa]	ΔP_c^s [Pa]	DEV
A7	1.78	490	0.6	330	420	21%
			3.1	420	500	16%
			13.8	420	500	16%
A8	1.70	264	1.1	877	790	-11%
			4.7	877	750	-17%
			12.0	877	840	-4%
A19	1.83	103	1.5	2720	2400	-13%
			3.1	2720	2410	-13%
			3.5	2720	2670	-2%
			10.0	2720	2450	-11%

Table 1: List of the tubes used in this work: tube ID, the main diameter D, the contraction diameter d, bubble length L, measured and simulated clogging pressure ΔP_c^m and ΔP_c^s, respectively, and the relative deviation DEV between them defined as DEV = $(\Delta P_c^s - \Delta P_c^m)/\Delta P_c^m$.

The tubes have typical internal main diameters D = 2 mm and contraction diameter d ranging between 100 and

500 µm. In a given experiment a single capillary tube was connected via stiff polymer (FEP) connection tubes to a syringe pump and a large reservoir, as shown in Figure 1. A single bubble was inserted in the tube and moved at steady flow rates ranging from 0.1 to 200 µL/s. Most experiments were performed at 0.33 µL/s to keep the laminar friction contribution to the pressure drops negligible. A MEMS-based piezoresistive differential pressure sensor (Honeywell 143PC03D with a response time of 1 ms and a resolution of ± 20 Pa) was connected through a Y-connection between the syringe pump and the tube. The sensor acquired the pressure difference across the bubble $\Delta P_b = P_{in} - P_{out}$, as shown in Figure 2, at a maximum sample rate of 100 Hz. The motion of the bubble was either observed through the stereo microscope visible in Figure 1, or through a microscope objective and a Firewire high-speed camera.

While performing experiments several precautions were taken to ensure that the measurements were reproducible. The interior of the glass tubes was soaked in a solution of 5% Contrad (Fisher Scientifics) overnight and then abundantly rinsed with deionized water. The wetting angles were measured for a bubble at equilibrium and for velocities corresponding to flow rates of 17.0, 3.33 and 0.33 µL/s, and their receding and advancing values were respectively 9° and 10°.

3 THEORY AND MODELING

A theoretical frame for interpreting our experimental results is provided by implementing the model for quasi-stationary motion of a gas bubble in a microchannel contraction discussed in [1] and adapting it to the channel geometries discussed in this paper. This model can be described as follows.

The pressure needed to move a bubble through a contraction of minimum diameter d, filled with a liquid of surface tension s is controlled by laminar friction and free surface forces. In quasi-static regimes, implying a low flow rate Q, the friction contribution is negligible, and a free surface contribution due to the Young-Laplace pressure appears when the bubble experiences changes in tube diameter or in its wetting properties changes [8]. The resulting pressure transient is proportional to s/d and may be several kPa: if the bubbles are large enough to span across the microchannel this may block the flow. The minimal external pressure needed to drive such bubbles out of the channel is called the clogging pressure ΔP_c.

On the basis of a microscope picture of a given tube a spline was fitted to obtain the shape of the contraction. This shape shown in Figure 2 is in turn used for numerical prediction of the pressure $\Delta P_b(x) = P_{in} - P_{out}$ across a bubble as a function of its position, where P_{in} and P_{out} are the pressure at the tube inlet and outlet, respectively, the latter being atmospheric pressure. A bubble is defined by its volume V_b and the value of the receding (left) and advancing (right) contact angles, q_L and q_R, at the contact lines of the left and right menisci, respectively. The total pressure drop ΔP_b is therefore:

$$\Delta P_b = P_{in} - P_{out} = 2s\left(\frac{\cos(q_R - q_t(x_R))}{r(x_R)} - \frac{\cos(q_L - q_t(x_L))}{r(x_L)}\right) \quad (1)$$

where $q_t(x)$ is the local tapering angle of the tube shape $r(x)$, a is a factor close to unity that depends on the shape of the contraction, β is a constant between unity (for a bubble outside the contraction) and zero (for a bubble spanning the contraction), and l_{con} is the length of the contraction. We find that this quasi-static model is in good agreement with most of our observations, and in the cases of deviations from experiments it is used as a starting point for pointing out possible theoretical improvements.

4 RESULTS AND DISCUSSION

In the following we present how the transient bubble pressure is influenced by four factors: *interface curvature, bubble breakup, tube diameter and flow rate*.

4.1 Influence of interface curvature

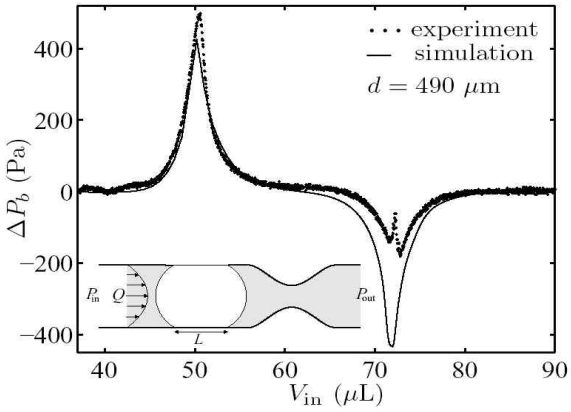

Figure 2: Direct measurement (dots) and simulation (full line) of the pressure across a long L = 8 mm bubble in tube A7 for Q = 0.33 µL/s as a function of displaced liquid volume $V_{in} = Q_t$, where t is the time. The differential pressure sensor measures $\Delta P_b = P_{in} - P_{out}$. The inset indicates the bubble length L, the liquid flow rate Q and the pressures P_{in} and P_{out}.

In Figure 2 is shown the measured and simulated pressure drop $\Delta P_b = P_{in} - P_{out}$ across the bubble, according to the definition of equation 1, as a function of the displaced liquid volume in the tube. Two peaks are seen: a positive one at V_{in}=51 µL and a negative one at V_{in}=72 µL. They correspond to the passage through the contraction of the left and right bubble meniscus, respectively. Before and after the two menisci have passed the contraction, the pressure difference across the bubble nearly vanishes, because the advancing and receding wetting angles are equal at such low capillary number, and only the negligible laminar viscous contribution remains.

In the simulation the two peaks are symmetrical. For the first peak, the agreement between the measured and simulated pressure is good, with comparable peak heights (within 20%), widths (5 μL) and shape. The magnitude of the second (negative) pressure peak is much smaller in the measurement than in the simulation, and a small pressure spike is visible around 72 μL. Two possible reasons for these are (1) that a thin liquid film between the bubble and the glass participates significantly in the pressure drop, and (2) that the rear meniscus of the bubble is pinned by interactions with impurities on the glass surface, or by interactions with a film left by the front meniscus. Since the measured values of the advancing and receding wetting angle were relatively low, our system can be considered as hydrophilic. It is therefore worth investigating if a thin water film formed along the bubble interacts with the two menisci of the moving bubble. The thickness h of a film left behind a fully-wetting meniscus moving at velocity U with low capillary number $Ca = \mu U/s$ in a tube of radius r, can be described by the Bretherton law [9], as $h/r \sim Ca^{2/3}$. For tubes with diameters of 2.0 to 0.1 mm, the flow rate of 0.33 μL/s corresponds to a meniscus velocity U = 0.1 to 40 mm/s and $Ca = 10^{-6}$ to 5×10^{-4}. The thickness h of the water film left behind is therefore between 200 and 600 nm. The presence of a thin film has been verified by observing temporal changes of interferences of white light with the bubble-tube contact surface. This transient phenomenon is likely to indicate the presence of a thin film and its dewetting. The second hypothesis, i.e., that the rear meniscus is flattened by pinning, was invalidated by visualizing with a high-speed camera the evolution of the menisci curvature.

4.2 Influence of bubble breakup

Experiments have been made with a tube exhibiting a narrower contraction (tube A19, 110 μm contraction), as shown in Figure 3. The viscous pressure drop, neglected in the modeling, is now significant and explains the difference in the base level of experimental and theoretical curve. The magnitude of the first pressure peak is comparable with the numerical simulation, however the shape is not in a good agreement with the simulation. This discrepancy arises because the FEP tubing and glass syringe in the measurement system are less stiff than the microbubble, a counterintuitive fact. Also, oscillations of the pressure occur at well-defined volume steps ΔV_{in} during the entire phase where the bubble is spanning the contraction. The saw-tooth pressure profile is due to capillary instabilities occurring when the bubble passes through a long contraction with large aspect ratio: the single bubble breaks into several smaller bubbles that merge back and separate again with a given frequency. This mechanism has been visualized and measured at 600 frames/second: it instability involves the creation and destruction of interfaces and induces saw-tooth perturbations in the pressure measurement. Comparison between timed images and measured pressure in Figure 3 indicates a good agreement in terms of the period ΔV_{in} = 0.54 μL of the perturbation.

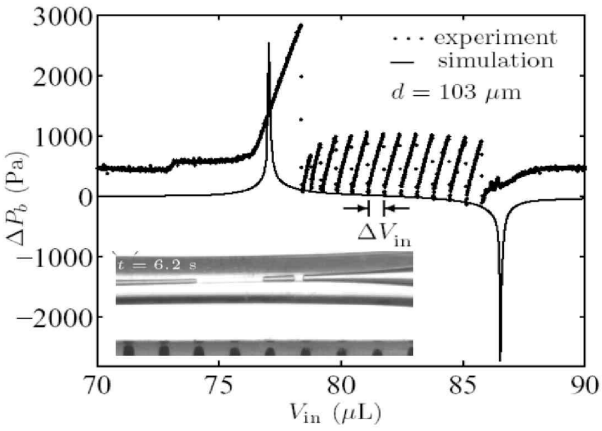

Figure 3: Measurements (dots) and simulation (full line) of the pressure drop ΔP_b across a L = 3.1 mm bubble in tube A19 for Q = 0.33 μL/s as a function of displaced liquid volume $V_{in} = Q_t$.

4.3 Influence of tube diameter

We define the minimum pressure ΔP_c needed to push a bubble through the contraction as the *clogging pressure*[1], and measure it for tubes with different contraction diameters, and for different length L of the bubbles. The results are summarized in table 1. The tubes have contraction diameters d between 103 and 490 μm, and the corresponding range of clogging pressure ΔP_c is from 2.7 to 0.3 kPa. The experimental and numerical pressure values agree within 20%. For a given contraction the amplitude of the first pressure peak is constant for bubbles larger than the contraction length. For small bubbles the amplitude of the first pressure peak is reduced because both menisci are in the contraction when the pressure reaches its maximum value [1].

4.4 Influence of the liquid flow rate

A long L = 10 mm bubble was moved in tubes A7, A8, and A19 with contraction diameters of 490, 264 and 103 μm, respectively, at flow rates ranging from 0.1 to 160 μL/s. The maximum amplitude ΔP of the positive and negative pressure peaks observed as the bubble passes through each contraction are plotted in Figure 4a as a function of the flow rate Q .Two regimes are visible in Figure 4a: (*i*) for flow rates smaller than a critical value, which depends on the contraction diameter, the positive and negative pressure peak amplitudes are constant, the positive peak being slightly larger than the negative one, as, e.g., in Figure 2. (*ii*) For flow rates larger than the critical value, the amplitude of the positive pressure peak decreases and ultimately vanishes, while the value of the negative pressure peak increases exponentially, without bound. This means that in this high flow-rate regime the bubble is easier

to push through the contraction. This is explained as follows: the first (positive) pressure peak when the bubble is pushed through the contraction is due at low flow rates to the Laplace pressure, and can be approximated by $\Delta P_s = 4s/d$. However, at higher flow rates an additional and opposite pressure drop due to difference of viscous losses between air and water arises as $\Delta P_{fric} = 128 m l_{con} Q/(\pi d^4)$. The observed change in regime, where the positive pressure-peak transient vanishes, therefore occurs when $\Delta P_{fric} = \Delta P_s$. Using this together with the expressions for the flow rate, $Q = \pi(d/2)^2 v$, and the capillary number, $Ca = \mu v/s$, the transition condition can be written as $Ca = d/8l_{con}$. Based on this equation it is convenient now to define a re-scaled capillary number Ca* as $Ca^* = Ca \cdot 8 l_{con}/d$. In terms of the re-scaled capillary number the transition happens at Ca* ˜ 1. Likewise, it is convenient to introduce the re-scaled pressure drop amplitude of the pressure transient $\Delta P^* = P(Q)/P(Q=0)$, i.e. the ratio between the observed amplitude of the transient pressure drop at high flow rate Q and the amplitude of the positive pressure transient at negligible flow rate $Q = 0$.

In Figure 4b the data of panel (a) are re-plotted using the re-scaled variables ΔP^* and Ca^*. It is seen how the transition between the capillary pressure drop regime, with a large positive peak amplitude, and the viscous pressure drop regime, with a vanishing positive peak amplitude, occurs for Ca^* ˜ 1. In other words, this criterion has practical implications: it discriminates between the case of bubbles clogging the flow through the contraction or not.

5 CONCLUSION

An experimental study of a bubble passing through a microchannel contraction has been performed. Transient measurements have quantified the pressure and bubble shape during its motion through the contraction. The experiments were confronted with the simple theoretical model of quasi-static motion, and generally a good agreement was obtained. However, some deviations have been observed and discussed. High-speed visualization reveal that some departures from the simulations are due to instabilities and break-up of the bubble. Experiments varying the flow rate show that two regimes govern the pressure transients when the bubble passes the contraction: a quasi-steady regime for low capillary number, and a viscosity-influenced regime for non-negligible capillary numbers. A criterion based on a modified capillary number is proposed to discriminate between these two regimes, and it shows the existence of a critical flush velocity above which clogging by bubbles at contractions is suppressed.

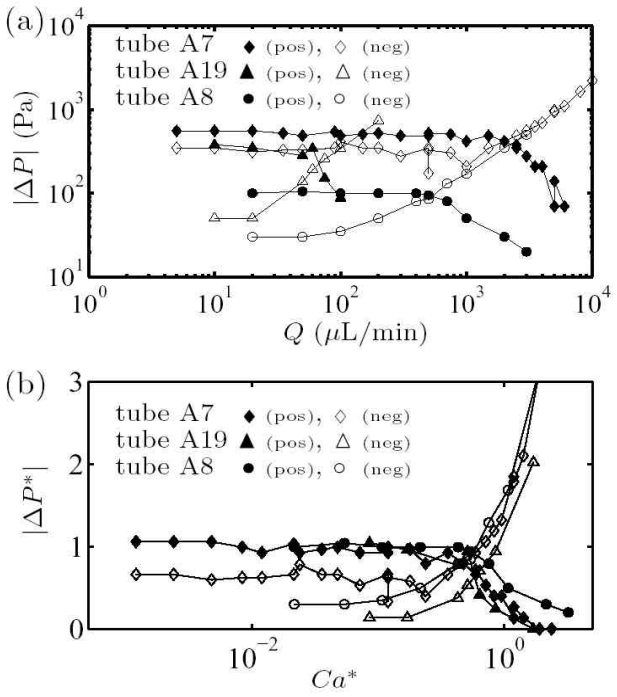

Figure 4: (a) Maximum amplitude ΔP of the positive (pos) and negative (neg) pressure peak observed as the bubble passes through the contraction versus flow rate Q for a long $L = 10$ mm bubble tubes A7, A8, and A19 with contraction diameters of 490, 264 and 103μm, respectively. (b) Same data as in panel (a), but now expressed in terms of the re-scaled variables ΔP^* versus Ca^*. The negative pressure peak is represented by the open symbols and the positive pressure peak by the filled symbols.

REFERENCES

[1] M. J. Jensen, G. Goranovic, and H. Bruus, J. Micromech. Microeng. 14, 876, 2004.

[2] O. Geschke, H. Klank, and P. T. (Eds.), "Microsystem Engineering of Lab-on-a-chip devices," Wiley-VCH, Weinheim, 2004.

[3] J. Tsai, L. Lin, and 97-98, Sensors and Actuators A, 97, 2002.

[4] A. Utada, E. Lorenceau, D. Link, et al., Science. 308, 537, 2005.

[5] S. Anna, N. Bontoux, and H. Stone, App. Phys. Lett. 364, 2003.

[6] P. Gravesen, J. Branebjerg, and O. S. Jensen, J. Micromech. Microeng. 3, 168, 1993.

[7] M. Elwenspoek, T. S. Kannerubj, R. Miyake, et al., J. Micromech. Microeng. 4, 227, 1994.

[8] G. K. Batchelor, "An Introduction to Fluid Dynamics," University Press, Cambridge, New York, 1967.

[9] F. Bretherton, Journal Fluid Mechanics. 10, 166, 1961.